

# Thermal Interface Conductance of Realistic Bolted Joints in Vacuum Environment

Sujana N<sup>a,\*</sup>, Dr. Amrit Ambirajan<sup>b</sup>, Dr.N.Shanmughapriya<sup>a</sup>.

<sup>a</sup>Department of Mechanical Engineering, Siddaganga Institute of Technology, Tumkuru - 572103, Karnataka.

<sup>b</sup>ISAC-ISRO, Bangalore

## Abstract

Conduction is the process of heat transmission from one medium to another medium; this plays a vital role in the space environment. The heat will be generated from the spacecraft's electronic box, which should flow from the conducting medium to the box surface. In contrast, it must either radiated or conducted to the heat sink. Therefore, the study of contact conductance is an important phenomenon; hence, this article deals with temperature and pressure variations /distribution between mating surfaces when two different thickness plates are brought together and joined using M4 bolts in a vacuum environment and correlated with analytical results.

**Keywords** - Thermal interface conductance, realistic bolted joints, vacuum environment, space environment, aluminum 6061, micro capsulated sheet, mikic relation.

## I. INTRODUCTION

Thermal contact conductance is the ability to conduct heat between two Solid bodies when they are in thermal contact, and the Inverse property of thermal contact conductance is called thermal contact resistance. (V. Madhusudana 1996)

$$H = \frac{Q/A}{T}, \quad R = \frac{A * T}{Q}$$

Cooper et al. [1969] developed an extrapolation method by extending the single circular contact hypothesis to multiple contacts with a distribution of asperity heights derived from surface topography measurements. Mikic [1974] also proposed a simple correlation to calculate thermal contact conductance.

$$\frac{h}{k} = 1.45 \left\{ \frac{P}{H} \right\}^{0.985}$$

Where,

h- Thermal conductance,

k- Thermal conductivity of the material

P-pressure applied

H- Hardness number

Singhal et al. (2005) developed a coupled thermo-mechanical predictive model to predict the actual contact area used in the computation of contact conductance; they predicted the contact between two rough surfaces with equivalent characteristics. In addition, they developed the surface topography

model in their study, which is tedious and difficult to use. Louis J Salerno et al. (1997) investigated the same but to find interface conductance by coating the bulk materials like Cu, Al, brass with Apiezon-NTM grease, Indium foil. It is observed that asymptotic leveling of the conductance increasing the thermal conductivity of the bulk materials. For thermal resistance, which is reciprocal of thermal conductance, Pavel V et al. (2015) conducted for the inverse heat conduction problem, which implies thermal properties (the thermal conductivity and thermal diffusivity), based on temperature and find the solution of the non-stationary direct problem with a point source of heat in the plane with the Laplace transform and the Fourier transforms.

These conductance experiments extended in the field of spacecraft, whereas in satellites, the heat generated from electronic components must be transferred to the outer surface of the structure through conduction and radiation medium to keep the temperature of the electronic components within acceptable levels (ALBIN K J. HASSELSTRÖM-2012). With lack of heat transfer through convection, and the influencing physical parameters. Ms. Kumkum B. Chauhan et al .reviewed the Influencing Parameters of Thermal Contact Resistance in 2017 and concluded that thermal conductance majorly depends on various parameter like the geometry of surface and hardness, interface material, contact thickness, the variance of pressure distribution in a bolted joint, Therefore, thermal management is considered a key issue in spacecraft and Determining thermal contact conductance in bolted joints is a major challenge when designing for space application. At the time of this thesis, models describing thermal contact conductance in bolted joints Contact gap, the pressure distribution is considered. And estimate the temperature distribution of the heater plate by numerically using UG-NX software over the interface as a different heat load and the different cold plate temperature.

## II. PRESSURE ANALYSIS

Before you begin to format your paper, first write, and the Baseplate and top plate are the components, made of aluminium6061. Lugs or bolts are used to tightening the heater plate with the source plate to bring the exact contact between the two plates. This heater plate is fixed to the source plate using an M4 bolt with a torque of 18 kgf-cm per bolt; Pressure is analyzed using pressure-sensitive film. When



pressure is applied, the microcapsules are broken, and the developing material reacts with color-forming materials reacting with the colour-developing material to make red. The microcapsules are designed to break according to pressure, so the color density corresponds to the pressure, as shown in fig below.

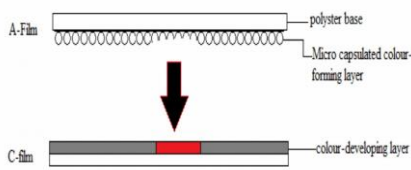


Fig: Effect of the film after applying pressure

The red color density of pre-scale changes depending on the amount of pressure applied. The area with deep red color indicates that the pressure applied was high, and conversely, the area with a light red color indicates that the pressure applied was low. Place the pre-scale on a few white sheets of paper with its smooth surface on top and check the light's result. The pre-scale on a few white sheets of paper with its smooth surface on top is scanned using special software and determined the pressure.

### III. EXPERIMENT

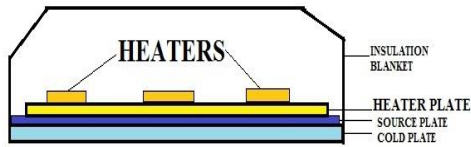
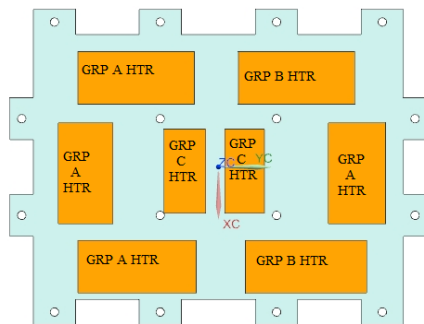


Fig: Experimental setup

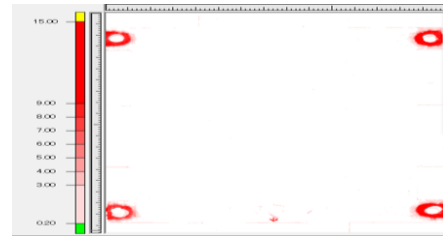
### IV. TEMPERATURE ANALYSIS



For temperature analysis, the bolts were inserted and tightened according to the specifications of the test cycle. The test specimens were clamped to the base plate and kept in the required vacuum environment  $1.3 \times 10^{-4}$  m bar. The sensors mounted, and the heater was connected through cables to the data processor and power supply. Specific amounts of power were applied on the heater in a sequence still it approaches steady state then to required test, and the temperatures of each sensor had been tabulated.

A numerical study was done using UG-NX software for test cycle boundary conditions. The obtained results were correlated with the experimental data.

### V. RESULTS AND DISCUSSIONS



The pressure is there only in the vicinity of bolts indicating that there is no proper contact for the rest of the area.

MIC1C: sim1: 1291: CASE: 1 H: 20192 Result  
Load Case 1: Static Step 1  
Temperature: Postfil: Scalar  
Min: -45.00, Max: -19.55, Units = C

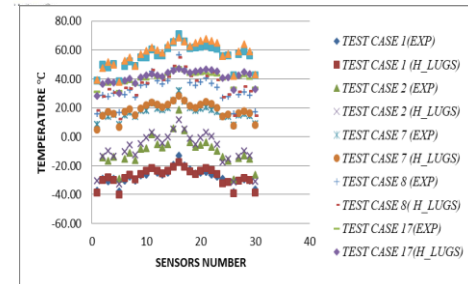
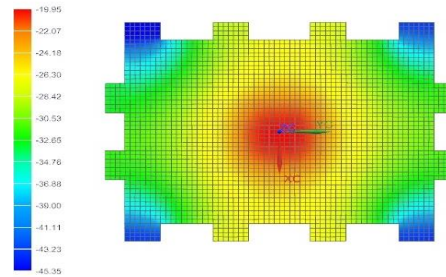
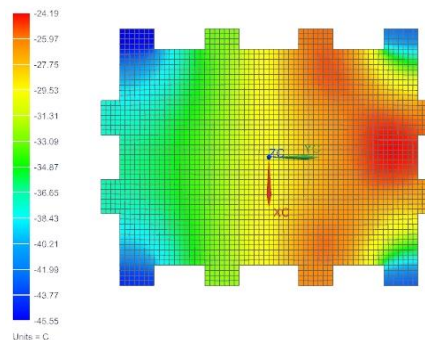
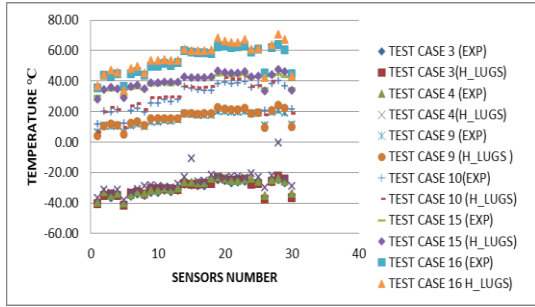


Fig: Temperature distribution on the heater plate with Group C heater is ON.

The above graph shows the comparison between experimental and numerical temperature with the heat-transfer coefficient  $8000 \text{ W/m}^2\text{K}$  [using B. Mikic, M. Yovanovich relation (3)] it shows the similar values as experimental when group C heater is ON. The maximum temperature is found in the heater region for different cold plate temperatures ( $-50^\circ\text{C}$ ,  $0^\circ\text{C}$ , and  $+25^\circ\text{C}$ ) for thermal loads (20W and 40W).





**Fig: Temperature distribution on the heater plate with Group B Heater is ON**

The above graph compares experimental and numerical temperature with the heat-transfer coefficient  $8000\text{W/m}^2\text{K}$  (using B. Mikic, M. Yovanovich relation 3). It shows similar values as experimental when group B heater is ON. The maximum temperature is found in the heater region for different cold plate temperatures ( $-50^\circ\text{C}$ ,  $0^\circ\text{C}$ , and  $+25^\circ\text{C}$ ) for thermal loads (20W and 40W).

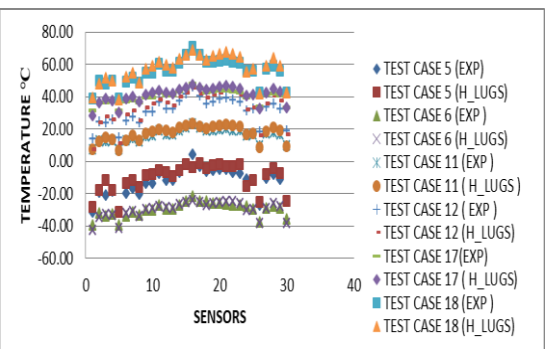
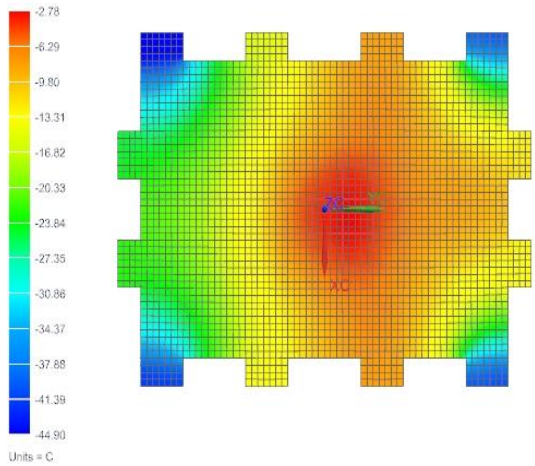


**Fig: Temperature distribution on the heater plate with Group B & C Heater is ON**

The above graph shows the comparison between experimental and numerical temperature with the heat-transfer coefficient  $8000\text{W/m}^2\text{K}$  [using B. Mikic, M. Yovanovich relation (3)] it shows the similar values as experimental when group B & C heater is ON. The maximum temperature is found in the heater region for different cold plate temperatures ( $-50^\circ\text{C}$ ,  $0^\circ\text{C}$ , and  $+25^\circ\text{C}$ ) for thermal loads (20W and 40W).

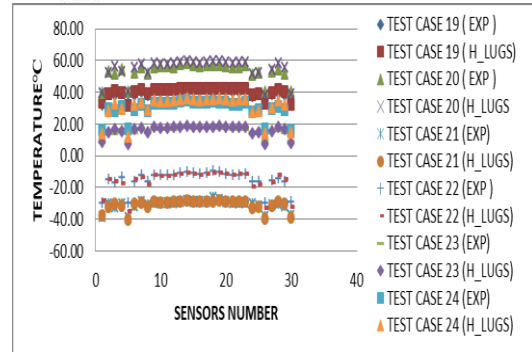
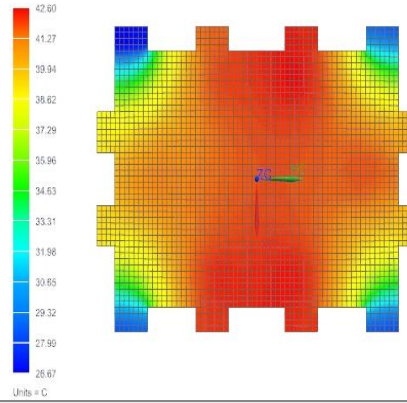


**Fig: Temperature distribution on the heater plate with Group A & B Heater is ON**

The above graph shows the comparison between experimental and numerical temperature with the heat-transfer coefficient  $8000\text{W/m}^2\text{K}$  [using B. Mikic, M. Yovanovich relation (3)] it shows the similar values as experimental when group A & B heater is ON. The maximum temperature is found in the heater region for different cold plate temperatures ( $-50^\circ\text{C}$ ,  $0^\circ\text{C}$ , and  $+25^\circ\text{C}$ ) for thermal loads (20W and 40W).

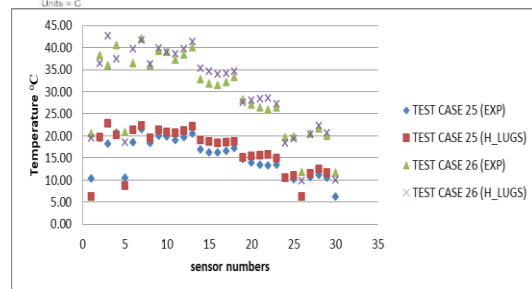
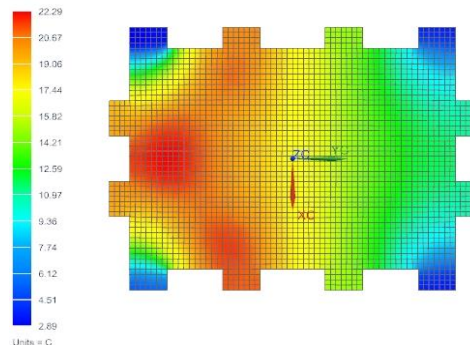


**Fig: Temperature distribution on the heater plate when Group A Heater is ON**

The above graph shows the comparison between experimental and numerical temperature with the heat-transfer coefficient 8000W/m2K [using B. Mikic, M. Yovanovich relation (3)] it shows the similar values as experimental when group A heater is ON. The maximum temperature is found in the heater region for different cold plate temperatures (-50°C, 0°C, and +25°C) for thermal loads (20Wand40W).

**EXPERIMENTAL AND TOTAL INTERFACE (NUMERICAL).**

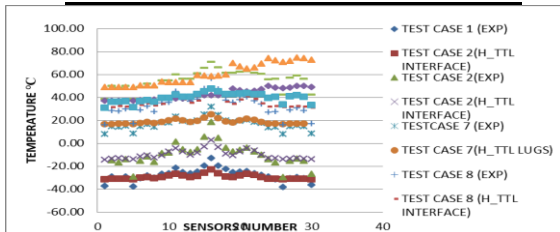
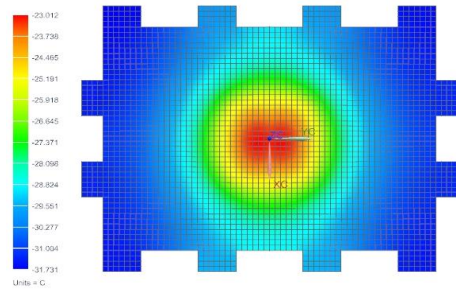


**Fig: Temperature distribution on the heater plate with Group C heater is ON.**

The above graph shows the comparison of the experimental temperature and numerical temperature where the heat-transfer coefficient 50W/m2K using [using B. Mikic, M. Yovanovich relation (3)] applied to complete interface (total interface) of the source and the heater plate, which shows the similar values as experimental when group C heater is ON. The maximum temperature is found near the heater region for different cold temperature -50°C, 0°C +25°C and thermal load 20W& 40W

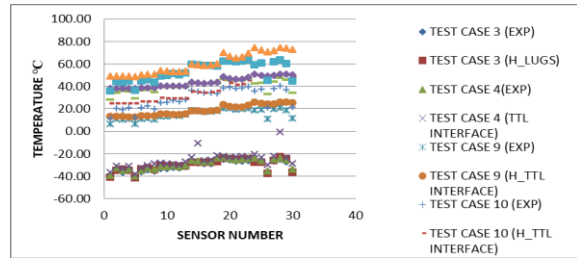
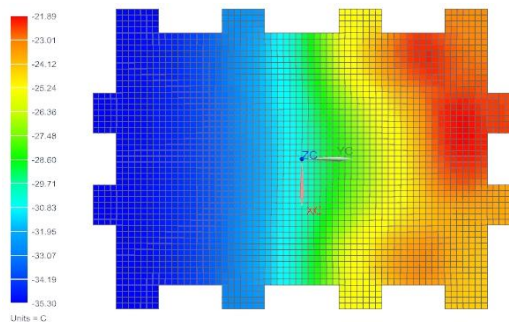


**Fig: Temperature distribution on the heater plate with Group B heater is ON.**

The above graph shows the comparison of the experimental temperature and numerical temperature where the heat-transfer coefficient 50W/m2K using [using B. Mikic, M. Yovanovich relation (3)] applied to complete interface (total interface) of the source and the heater plate, which shows the similar values as experimental when group B heater is ON. The maximum temperature is found near the heater region for different cold temperatures -50°C, 0°C +25°C, and thermal load 20W& 40W.

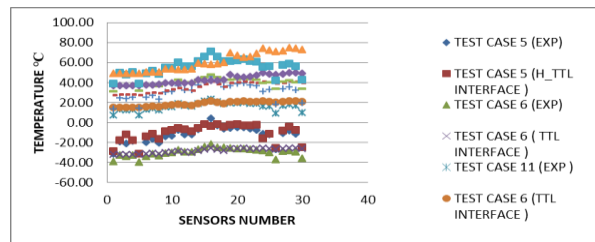
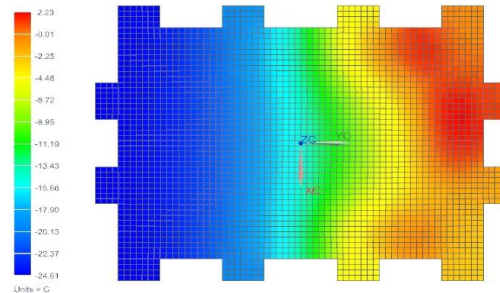


**Fig: Temperature distribution on the heater plate with Group B&C heater is ON.**

The above graph shows the correlation of the experimental temperature and numerical temperature where the heat-transfer coefficient 50W/m2K applied to complete interface (total interface) of the source and the heater plate, which shows the similar values as experimental when group B&C heater is ON. The maximum temperature is found near the heater region (middle left side of the plate) for different cold temperature -50°C, 0°C +25°C and thermal load 20W& 40W respectively and temperature found to be correlated

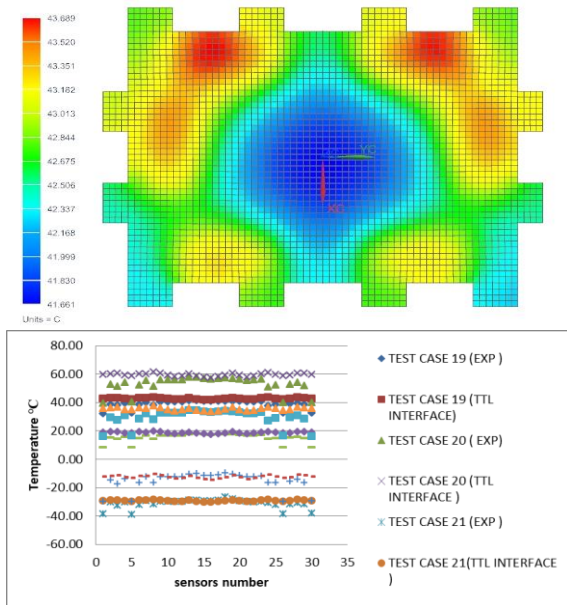


**Fig: Temperature distribution on the heater plate with Group A&B heater is ON.**

The above graph shows the comparison of the experimental temperature and numerical temperature where the heat-transfer coefficient  $50\text{W/m}^2\text{K}$  using [using B. Mikic, M. Yovanovich relation (3)] applied to complete interface (total interface) of the source and the heater plate, which shows the similar values as experimental when group A&B heater is ON. The maximum temperature is found near the heater region for different cold temperatures  $-50^\circ\text{C}$ ,  $0^\circ\text{C}$   $+25^\circ\text{C}$ , and thermal load  $20\text{W}$  &  $40\text{W}$ .

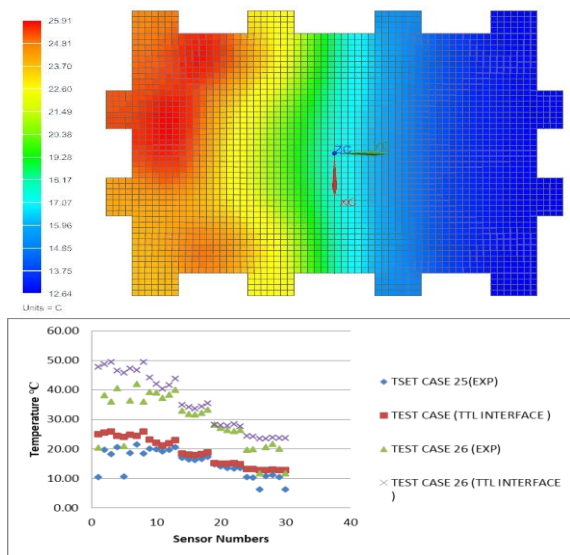


**Fig: Temperature distribution on the heater plate with Group A heater is ON.**

The above graph shows the comparison of the experimental temperature and numerical temperature where the heat-transfer coefficient  $50\text{W/m}^2\text{K}$  using [using B. Mikic, M. Yovanovich relation (3)] applied to complete interface (total interface) of the source and the heater plate, which shows the similar values

as experimental when group A heater is ON. The maximum temperature is found near the heater region for different cold temperature  $-50^\circ\text{C}$ ,  $0^\circ\text{C}$   $+25^\circ\text{C}$  and thermal load  $20\text{W}$  &  $40$

## VI. CONCLUSION

To study the temperature and pressure distribution in Al6061 used in spacecraft under vacuum environment. The following conclusion made from this work

1. Thermal contact conductance strongly depends on contact pressure, for bare joint contact is found around the bolted joint.
2. The contact conductance is significant only in the bolted region result in contact conductance and negligible in other contacts.
3. Temperature prediction using a contact conductance distribution derived from the pressure distribution was close to experimentally observed.
4. A high value of  $H = 8000\text{W/m}^2\text{K}$  only on bolted lugs and the rest of the area with zero conductance gives a good prediction.
5. Temperature prediction of the component assumes uniform contact conductance throughout the interface for  $50\text{W/m}^2\text{K}$  and significantly matches the experimental data.

## REFERENCES

- [1] "The parameters affecting on Thermal contact conductance-A Review" Ms. Kumkum B. Chauhan<sup>1</sup>, Prof. Hitesh R. Raiyani<sup>2</sup> 1M.E. Scholar, L.J. Institute of Engineering & Technology, Ahmedabad 2Assistant Professor, L.J. Institute of Engineering & Technology, Ahmedabad
- [2] "Thermal Conductance," Springer Publications, C.Madhusudana,1996
- [3] Shanmugan S, Mutharasu D "Thermal transient analysis of high power LED tested on Al<sub>2</sub>O<sub>3</sub> thin film coated Al substrate", International Journal of Engineering Trends and Technology (IJETT), V30(6),270-275 December 2015. ISSN:2231-5381.
- [4] "Thermal contact conductance": Louis J Salerno and peter Kittel, Ames Research center California(1997):
- [5] "Thermal contact conductance," M. Cooper, B. Mikic, M. Yovanovich Int. J. Heat Mass Transfer 12 (1969) 279–300.
- [6] "Thermal contact conductance; theoretical considerations," B. Mikic', Int. J. Heat Mass Transfer 17 (1974) 205–214.
- [7] "An Experimentally validated thermo-mechanical model for the prediction of thermal contact conductance" "Vishal Singhal, Paul J.Litke, Antony F. Black, Suresh V.Garimella cooling technologies Research center, school of mechanical engineering, Purdue University, West Lafayette, USA
- [8] "Estimation of thermal conductance on metallic contact interface in vacuum" T. ~attori', M. ~akamura' & Y. saitou<sup>2</sup> 'ech. Eng. Res. Lab., Hitachi Ltd., Japan 2~uclear System Division, Hitachi Ltd., Japan
- [9] "Determination of the Thermal Characteristics of Flat Solids" Pavel V. Balabanov, Vasily Pogonin, and Alexander N. Pchelintsev Tambov State Technical University ul. Sovetskaya 106, Tambov, 392000 Russian Federation.